


## Effects of climate and anthropogenic changes on current and future variability in flows in the So'o River Basin (south of Cameroon)

Valentin Brice Ebodé <sup>a,b,\*</sup>, Jean Guy Dzana<sup>a</sup>, Elias Nkiaka<sup>c</sup>, Bernadette Nka Nnomo<sup>d</sup>, Jean Jacques Braun<sup>b</sup> and Jean Riotte<sup>e</sup>

<sup>a</sup> Department of Geography, University of Yaounde 1, Yaounde, P.O. Box 755, Cameroon

<sup>b</sup> International Joint Laboratory DYCOFAC, IRGM-UY1-IRD, Yaounde BP 1857, Cameroon

<sup>c</sup> Department of Geography, University of Sheffield, Sheffield S10 2TN, South Yorkshire, UK

<sup>d</sup> Institute of Mining and Geological Research (IRGM), Hydrological Research Center, Yaounde, P.O. Box 4110, Cameroon

<sup>e</sup> Indo-French Cell for Water Sciences, Joint IRD-IISc Laboratory, Indian Institute of Science, Bangalore, India

\*Correspondence author. E-mail: ebodebriso@gmail.com

 VBE, 0000-0003-3307-4789

### ABSTRACT

Due to climate and environmental changes, sub-Saharan Africa (SSA) has experienced several drought and flood events in recent decades with serious consequences on the economy of the sub-region. In this context, the region needs to enhance its capacity in water resources management, based on both good knowledge of contemporary variations in river flows and reliable forecasts. The objective of this article was to study the evolution of current and future (near (2022–2060) and distant (2061–2100)) flows in the So'o River Basin (SRB) in Cameroon. To achieve this, the Pettitt and modified Mann–Kendall tests were used to analyze hydrometeorological time series in the basin. The Soil and Water Assessment Tool (SWAT) model was used to simulate the future flows in the SRB. The results obtained show that for the current period, the flows of the So'o decrease due to the decrease in precipitation. For future periods, a change in precipitation in line with the predictions of the CCCma model will lead to a decrease in river discharge in the basin, except under the RCP8.5 scenario during the second period (2061–2100), where we note an increase compared to the historical period of approximately +4%. Results from the RCA4 model project an increase in precipitation which will lead to an increase in river discharge by more than +50%, regardless of the period and the scenario considered. An increase in discharges was noted in some cases despite a drop in rainfall, particularly in the case of discharges simulated for the second period (2061–2100) from the outputs of the CCCma model. This seems to be a consequence of the increase in impervious spaces, all the more the runoff increases during this period according to the model. Results from this study could be used to enhance water resources management in the basin investigated and the region.

**Key words:** change in land use modes, climate change, current discharges, future discharges, regional climate models, southern Cameroon

### HIGHLIGHTS

- Impact of current climate change and anthropization on river discharge in equatorial central Africa.
- Impact of future climate change and anthropization on river discharge in equatorial central Africa.

## 1. INTRODUCTION

Variations in river flow generally result from interactions between climate change and/or anthropogenic changes (Diem *et al.* 2018; Oudin *et al.* 2018; Ebodé *et al.* 2021a). However, the study of the impact of these environmental forcings is done in different ways. In some works, this impact has been studied using the historical/contemporary period (Cissé *et al.* 2014; Bodian *et al.* 2020; Descroix *et al.* 2020). Meanwhile, other studies have addressed it over future periods to plan how available water resources will be distributed among different sectors (Abe *et al.* 2018; Fentaw *et al.* 2018; Dibaba *et al.* 2020). Until now, there are few studies (Ardoin-Bardin 2004; Sighomnou 2004) that have addressed both the study of the impact of environmental forcings on flows using current and future climate projections in some regions like Central Africa, due to the scarcity of data. The active network of this part of the continent now only includes 35 stations in the DRC (i.e. one station for 67,000 km<sup>2</sup>), 22 in Cameroon and less than 20 for all of Gabon, Congo and Central African Republic (Bigot *et al.* 2016).

This is an Open Access article distributed under the terms of the Creative Commons Attribution Licence (CC BY 4.0), which permits copying, adaptation and redistribution, provided the original work is properly cited (<http://creativecommons.org/licenses/by/4.0/>).

Such studies are urgently needed to assess the current and future evolution of water resources in a given region, in order to put in place different water management strategies.

In equatorial Central Africa, recent studies focusing on the impact of environmental forcings on flows during the historical period have highlighted a drop in average and extreme flows linked to a drop in rainfall for some basins such as the Ntem and the Ogooue (Conway *et al.* 2009; Ebodé *et al.* 2020; Ebodé *et al.* 2021b). In other basins such as the Nyong and the Mefou, it has been demonstrated that maximum flows may stay the same or increase, as a result of changes in land use patterns. These changes, which are essentially marked by an increase in impervious areas (buildings, roads and bare soil) to the detriment of the forest, would then compensate for the rainfall deficit by an increase in runoff, hence maximum flows will stay the same in the larger basins and increase in the smaller ones (Ebodé *et al.* 2022). In forested equatorial Central Africa, there are few studies addressing the impact of environmental forcings on flows during future periods using state-of-the-art methodology and new data (Akoko *et al.* 2021).

In other regions of the world, predictive hydrological modeling is done using a global or distributed/semi-distributed approach. The global approach considers the watershed as a single entity. The GR2J (Rural Engineering model with two daily parameters) and GR4J (Rural Engineering model with four daily parameters) models are some of the reference models generally used in this type of approach (Perrin *et al.* 2003; Bodian *et al.* 2012; Amoussou 2015). These models take into account parameters such as precipitation, evapotranspiration and soil water capacity. In the distributed/semi-distributed approach, on the other hand, the watershed is considered as a complex entity and flow modeling requires a subdivision into homogeneous elementary surfaces (Legesse *et al.* 2003; Githui *et al.* 2009; Taleb *et al.* 2019). Distributed/semi-distributed models require a wide range of input data, ranging from physical characteristics of the basin (slopes, land cover, soils, etc.) to meteorological data (precipitation, maximum and minimum temperatures, wind speed, relative humidity, insolation, etc.).

In terms of performance, the comparison of global and distributed/semi-distributed approaches in modeling is a problem that has been strongly developed for a long time (Wending 1992; Ague *et al.* 2014). Results from such model assessments provide a relatively complex picture as some authors clearly state the benefits of using the distributed/semi-distributed approach (Michaud & Soroshian 1994; Krysanova *et al.* 1999; Boyle *et al.* 2001) while other studies (Diermanse 1999; Kokkonen & Jakeman 2001) present opposite results. Some studies also show that the global approach gives better results in small watersheds, while the distributed/semi-distributed approach performs better in the case of large watersheds. These findings suggest that distributed/semi-distributed models are particularly applicable for complex watersheds due to their physical heterogeneity (Tegegne *et al.* 2017). Due to the complex nature of our study area, this study adopted a semi-distributed modeling approach considering that a previous study in the area using the lump conceptual modeling approach produced poor results (Sighomnou 2004). One of the complexities of the study area is the existence of two rainy seasons in the region.

In recent decades, several distributed/semi-distributed hydrological models have been developed to simulate the hydrological processes of watersheds and predict flows. Typical examples of distributed hydrological models include TOPMODEL (Topography-based Hydrological Model) (Beven & Kirkby 1979), SHE (European Hydrological System) (Abbott *et al.* 1986), Soil and Water Assessment Tool (SWAT) (Arnold *et al.* 1998), MGB-IPH (Large Basin Hydrological Model) (Collischonn & Tucci 2001), etc. Since the others only allow an approximate characterization of the physical environment of the watershed through the use of data and parameters in a point-grid network (Cao *et al.* 2006; Wang *et al.* 2012), SWAT appears to be the most efficient model in the wide range of applications.

The SWAT model has been widely used around the world for hydrological simulations of basins with different environmental conditions (climate, topography, geology, soils and vegetation) (Von Stackelberg *et al.* 2007; Pereira *et al.* 2010; Andrade *et al.* 2013) with satisfactory results obtained. For SWAT to become a universal hydrological model, more studies are needed in basins with climatic regimes and soils typical of equatorial conditions, such as that of the So'o basin in southern Cameroon.

The objectives of this study were to (1) evaluate the capacity of the SWAT model to simulate flows in a complex equatorial river basin with two rainy season regimes and (2) use the model to simulate future flows in the basin under different climate change scenarios. One of the biggest challenges to hydrological modeling in basins in the absence of sufficient flow gauging stations and the ability of the SWAT to simulate flows in this poorly gauged basin will be of great importance for socio-economic development considering the number of construction projects including dams and bridges ongoing in the basin. The results obtained could help to improve the management of water resources in this basin and the region.

## 2. MATERIALS AND METHODS

### 2.1. Study area

The study focuses on the So'o watershed (Nyong sub-basin) at the So'o bridge (1,934 km<sup>2</sup>). Beyond the fact that several socio-economic projects (dams, bridges, etc.) have been recently initiated in this basin, its choice is due to the fact that it is one of the few in the region with a recent series of flows and rainfall without gaps, which is an asset for this study. The So'o River Basin (SRB) is located in Central Africa between latitudes 2°50'N and 3°17'N, and longitudes 11°25'E and 11°38'E (Figure 1). It belongs to the sub-equatorial domain, with abundant rainfall (>1,600 mm/year). Rainfall is distributed over four seasons of unequal importance with two dry and two rainy seasons. The rainy seasons (spring and autumn) are generally very wet with average rainfall of about 900 mm and marked by numerous storms which sometimes cause major floods. The winter dry season is the only true dry season in the region, with average rainfall of about 90 mm, the summer dry season tending to become wetter in the region since the 1980s (Liénoú *et al.* 2008; EboDé *et al.* 2020). The So'o basin is dissected with deep gullies and cut into hills with convex slopes and wide marshy valleys (Olivry 1986). The geological substratum of the basin consists of a granito-gneissic base on which ferralitic (on the summits and slopes) and hydromorphic (in the lowlands) soils develop. The vegetation is dense semi-deciduous forest with Sterculiaceae and Ulmaceae strongly subject to anthropogenic actions (Letouzey 1985).

### 2.2. Data sources and methodology

#### 2.2.1. Data

**2.2.1.1. Spatial data.** The spatial data required for this study are of the following three types: a Digital Elevation Model (DEM), land use map and soil map.

DEM data used in this study have a spatial resolution of 30×30 m. It was obtained from the United States Geological Survey website (<https://earthexplorer.usgs.gov/>). The DEM was used to delineate the watershed, slope classification and to generate the hydrological response units (HRUs). In total, 33 HRUs were delineated in the SRB with slopes varying from 11 to 60% (48.5% of the total area of the basin). The dominant slope class is mostly found in the south of the basin (Figure 2). The slopes of 0–5% and 6–10%, respectively, occupy 18.6 and 32.9% of the watershed. These two slope classes are observed more in the northern and middle parts of the SRB (Figure 2).

The FAO world digital soil map downloaded from the site <http://www.fao.org/geonetwork/srv/en/metadata.show?id=14116> was used as soil data in this study. The soil classification used is based on the FAO classification system and was customized as required by the SWAT model (Figure 2). Three types of soils characteristic of the forest zone, namely the Orthic Ferralsols (Fo), have been identified in the basin (Fo1-ab-481, Fo26-ab-490 and Fo33-2ab-491). Types Fo26-ab-490 and Fo33-2ab-491 are the most widely represented with 46.7 and 53.2% of the whole basin.

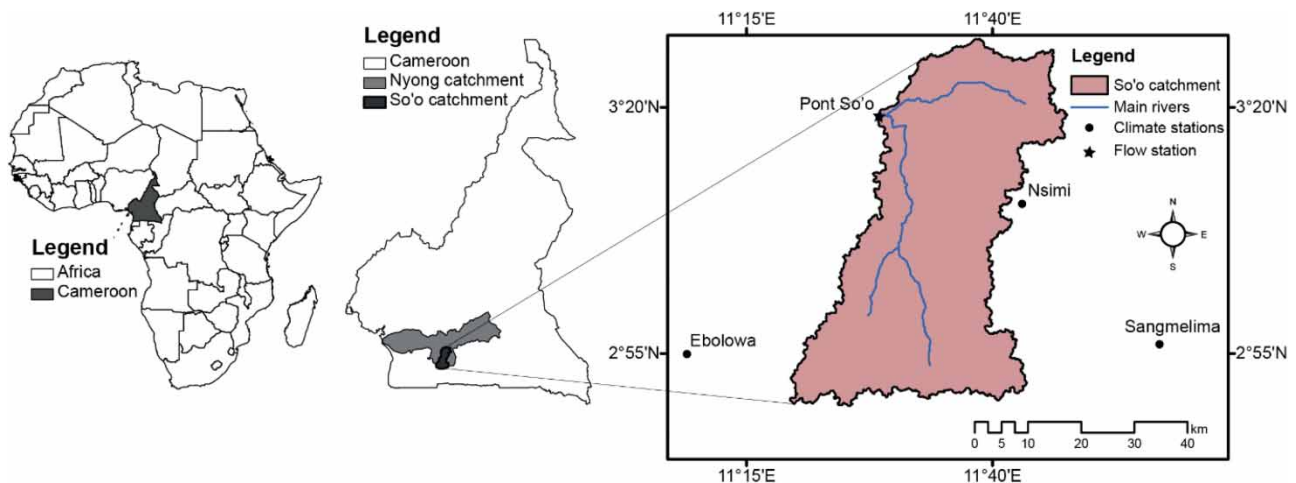


**Figure 1** | Location map of the So'o catchment at the So'o bridge.

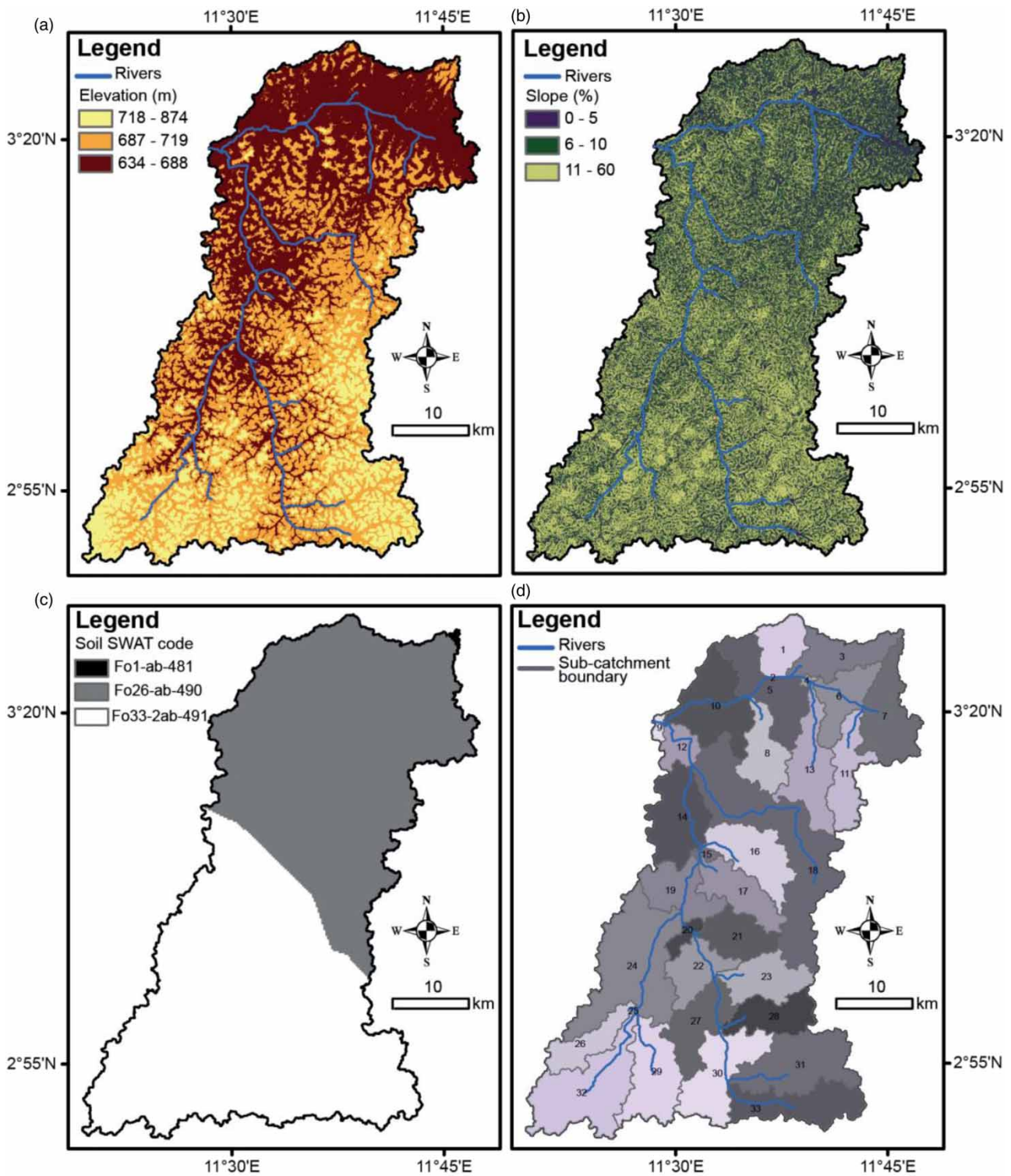


**Figure 2** | Elevation (a), slope (b), soil (c) and sub-basin (d) maps of the So'o catchment.

Apart from topographic and soil information which remain unchanged on the human time scale, the simulation of flows from the SWAT model requires other dynamic information such as land use. Three Landsat satellite images were used to produce land cover maps. These are the Landsat Thematic Mapper (TM) images of 2005, and Landsat 8 (OLI) of 2015 and 2020.

The maps produced from the images of 2005 and 2015 served as a reference in the QGIS software, to predict the land cover in 2035 and 2065. The 2020 map was used to validate the one simulated for the same year from the two previous ones (2005 and 2015 maps) since any prediction from a model requires calibration and validation of the said model. Similarly, the reliability of a model's outputs depends on the validation results of the model in question.

**2.2.1.2. Hydrometeorological data.** Rainfall data used to study the current period were obtained from the Climate Research Unit (CRU) of the University of East Anglia in the United Kingdom. The data are available from 1901, via the site [https://climexp.knmi.nl/selectfield\\_obs2.cgi?id=2833fad3fef1bedc6761d5cba64775f0/](https://climexp.knmi.nl/selectfield_obs2.cgi?id=2833fad3fef1bedc6761d5cba64775f0/) in NetCDF format, on a monthly time step and at a spatial resolution of  $0.25^\circ \times 0.25^\circ$ . The flow series used is that of ORE-BVET (Environmental Research Observatory/Tropical Experimental Watersheds).

The following meteorological data are for modeling flows in SWAT at daily time step: maximum and minimum temperatures ( $^\circ\text{C}$ ), precipitation (mm/day), relative humidity (%), average wind speed (m/s) and solar radiation (in  $\text{W}/\text{m}^2$ ). Among all these variables, only rainfall was observed at the selected stations (Nsimi, Ebolowa and Sangmelima) (Figure 1). Precipitation data were obtained from the meteorological service of the Ministry of Transport in Cameroon. The other variables were uploaded to these same stations on the SWAT website (<https://globalweather.tamu.edu/>). These are data from the National Centers for Environmental Prediction (NCEP). It has been shown that these data could constitute a good alternative for modeling flows in ungauged regions (Dile *et al.* 2013; Fuka *et al.* 2013; Nkiaka *et al.* 2017). All the meteorological data used were collected over the period 1998–2008.

### 2.2.2. Analysis of hydrological and rainfall data from the contemporary period

The analysis of average rainfall and flow was carried out using Pettitt (Pettitt 1979) and modified Mann–Kendall (Hirsch & Slack 1984; Araghi *et al.* 2014) statistical tests at the 95% significance level. Following the application of autocorrelation (from the calculation of the R statistic) and seasonality (from the employment of the correlogram) tests to the rainfall and flow series used, it turned out that there is a seasonality in the latter. It is why we chose to use the modified Mann–Kendall test of Hirsch & Slack (1984) to the detriment of the classic Mann–Kendall test and other modified Mann–Kendall tests.

The principle of the Pettitt test consists in dividing the series studied (of number  $N$ ) into two sub-samples of sizes  $m$  and  $n$ , respectively. We then calculate the sum of the ranks of the elements of each sub-sample in the total sample. A statistical study is then carried out from the two sums thus determined, then it is tested according to the hypothesis that the two sub-samples do not belong to the same population. Pettitt's test is non-parametric and derives from Mann–Whitney's test. The absence of a break in the series ( $X_i$ ) of size  $N$  constitutes the null hypothesis. Its implementation assumes that for any time  $T$  between 1 and  $N$ , the time series ( $X_i$ )  $i-1$  to  $t$  and  $t+1$  to  $N$  belong to the same population. The variable to be tested is the maximum in the absolute value of the variable  $U_t, N$  defined by:

$$U_t, N = \sum_{i=1}^t \sum_{j=t+1}^N D_{ij}$$

where  $D_{ij} = \text{Sign}(x_i - x_j)$  with  $\text{Sign}(x) = 1$  if  $x > 0$ , 0 and  $-1$  if  $x < 0$ .

If the null hypothesis is rejected, an estimate of the break date is given by the instant defining the maximum in absolute value of the variable  $U_t, N$ .

The Mann–Kendall test statistic for each season is calculated as follows:

$$S_g = \sum_{i < j} \text{Sign}(x_{jg} - x_{ig}) \quad g = 1, 2, \dots, p$$

The seasonal Kendall statistic is calculated as follows:

$$s' = \sum_{g=1}^p S_g$$

There is no significant trend in the series analyzed when the calculated  $p$ -value is above the chosen significance level. More details on the modified version of the Mann–Kendall test can be found in the relevant literature (Hirsch & Slack 1984).

### 2.2.3. Assessment of the impact of climate change and land-use patterns on runoff

The response of discharges from the So'o watershed to climate change and anthropization was assessed over two future periods (2022–2060 and 2061–2100). The interval 1999–2008 served as the reference/historical period. Rainfall data of the station used are without gaps over this interval. The 2005 land cover map was used to simulate runoff for the reference period (1999–2008). Those simulated for the years 2035 and 2065 were, respectively, used to simulate basin flows in the near (2022–2060) and distant (2061–2100) future.

### 2.2.4. Modeling changes in land-use patterns

Cellular automata (CA)–Markov is the procedure used for land cover prediction in this work. It combines Markov chains (quantity), multi-criteria evaluation (location) and filtering. This procedure is described as CA (Halmy *et al.* 2015). Markovian chains analyze two images of land cover at different dates and produce two transition matrices (probability and affected area in pixels for persistence and transition), and a set of conditional probability images. They make it possible to calculate a future state from the known present state, based on the observation of past evolutions and their probability. This makes this method one of the best for modeling the temporal and spatial dimensions of land use patterns (Halmy *et al.* 2015; Yang *et al.* 2019).

The performance of the CA–Markov model in predicting land cover maps was evaluated using Kappa coefficients calculated by the equation:

$$\text{Kappa} = \frac{Po - Pc}{1 - Pc}$$

where  $Po$  is the proportion of correctly simulated cells;  $Pc$  is the expected proportion correction by chance between the observed and simulated map. If the Kappa index  $\leq 0.5$ , this indicates poor proximity between the two compared cards (simulated and observed). If  $0.5 \leq \text{Kappa} \leq 0.75$ , the proximity between the two maps is acceptable. When  $0.75 \leq \text{Kappa} \leq 1$ , the proximity between the two maps is good. When  $\text{Kappa} = 1$ , the two cards are identical. The Kappa coefficient obtained for the comparison between the observed and simulated maps for the year 2020 in this study is 0.87, which gives credibility to the simulated maps for the years 2035 and 2065.

### 2.2.5. Climate change scenarios

In this study, two regional climate models (RCMs) [RCA4 and CCCma] from the CORDEX project that have proven to be effective in simulating precipitation and temperature in Africa (Gadissa *et al.* 2018; Dibaba *et al.* 2019) were retained. However, despite their reliability and the degree of confidence that can be granted to them, the outputs of the models sometimes present considerable biases, which require corrections before using them to study the impact of climate change. For each of the RCMs, data from two scenarios (RCP4.5 and RCP8.5) were collected. The first and second scenarios are, respectively, representative of high greenhouse gas emissions and moderate emissions. The other meteorological variables (solar radiation, relative humidity and wind speed) considered for the historical period have been taken over for the two future periods without making any changes, given that their modifications have no significant impact on the modeling result (Gadissa *et al.* 2018).

### 2.2.6. Bias correction

Climate Model Data for Hydrological Modeling (CMhyd) software (Rathjens *et al.* 2016) obtained from <https://swat.tamu.edu/software/> was used to correct for precipitation and temperature biases. Teutschbein & Seibert (2012) provided a comprehensive review of bias correction techniques based on this tool. According to the authors, all the correction techniques improved the simulations of precipitation and temperature. However, they noted differences between the correction methods. Based on the proximity between the corrected datasets and the observed datasets, distribution mapping (DM) was considered to be the best correction method, both for temperature and precipitation. According to the authors, DM uses a transfer function to adjust the cumulative distribution of the corrected data to that of the observed data, which makes the results significantly better. Zhang *et al.* (2018) compared five bias correction methods using the CMhyd tool. They demonstrated that DM was the most efficient correction method for studying the impact of climate change on the flow dynamics of two rivers in the northern basin of Lake Erie (Canada). Based on these results, DM was retained for the precipitation and temperature corrections of the model outputs used in this study.

### 2.2.7. SWAT model description

SWAT is a physically based semi-distributed hydrological model, designed and developed by researchers at the USDA (United States Department of Agriculture) (Arnold *et al.* 1998). The physical aspect of the model makes it possible to reproduce the processes that take place in the environment, using different sets of equations (Neitsch *et al.* 2005; Arnold *et al.* 2012). This model is continuous over time and is designed to run simulations over long periods (Payraudeau 2002). The SWAT model analyzes the watershed as a whole by subdividing it into sub-watersheds containing homogeneous portions called HRUs. Each HRU is characterized by unique land use, soil type and topography. SWAT provides access to the different water balance components at the HRU scale for each time step (daily, monthly and annual) over the simulation period (Neitsch *et al.* 2005).

### 2.2.8. Model evaluation criteria

The validity of a hydrological model was checked by comparing the model simulated ( $Q_{sim}$ ) ( $Q_{cal}$ ) and observed ( $Q_{obs}$ ) flows through subjective and quantitative criteria. Initially, a good match between the observed and simulated flow hydrographs will attest to good calibration. In the second step, we used three of the most widely used criteria for the validation of hydrological models, correlation coefficient ( $r$ ), the Nash index ( $NSE$ ) and the bias (Akoko *et al.* 2020).

The correlation coefficient is the ratio between the covariance ( $\gamma$ ) of two variables and the product of their standard deviations. It indicates the intensity and direction of the linear relationship between two variables. Varying between  $-1$  and  $+1$ , it reflects a strong correlation if it is less than  $-0.5$  or greater than  $0.5$ .

$$r = \frac{\gamma(X, Y)}{\sigma_X \sigma_Y}$$

The Nash–Sutcliffe criterion gives a ratio of the squared difference between the observations and the estimates to relate them to a deviation from the mean of the observations. It varies between 0 and 1. When the Nash criterion is equal to 1, the estimates are identical to the observations. When it is 0, it is considered that the model is no better than if we had taken, at each time step, the temporal average of the observations.

$$\text{Nash} = 1 - \frac{\sum (Q_{sim} - Q_{obs})^2}{\sum (Q_{obs} - \overline{Q_{obs}})^2}$$

The bias is the ratio of the difference between the observations and the estimates, and the observations. It indicates a percentage of the overestimation or underestimation of generally unobserved data compared to observations.

$$\text{Bias} = 100 \frac{\sum_{i=1}^N (Q_{est,i} - Q_{obs,i})}{\sum_{i=1}^N Q_{obs,i}}$$

## 3. RESULTS AND DISCUSSION

### 3.1. Current hydroclimatic variability

#### 3.1.1. Interannual and spatial evolution of precipitation

Annual and seasonal rainfall in the SRB decreased over the period 1998–1999 to 2018–2019. However, this decrease is not significant according to the Pettitt and Mann–Kendall tests (Figure 3). If we stick to the slopes of the regression lines and the calculated  $p$ -values, the precipitation of the two rainy seasons recorded the largest (autumn) and least (spring) decrease, respectively. This study notes a decrease in summer rainfall, which contrasts with previous studies conducted in the region (Liéno *et al.* 2008; Ebodé *et al.* 2020), in which an increase in summer precipitation was highlighted. This could be explained by the period chosen for this study (1998–1999 to 2018–2019). The data sets used in previous studies started in the 1950s.

Spatially, this decrease is from the East to the West of the basin for annual and seasonal precipitation (Figure 4). For annual rainfall, for example, the lowest rainfall class, which was essentially confined to the northeast of the basin during the 2000s, covered almost the entire basin during the 2010s (Figure 4). The rainfall of the summer dry season decreases from South to North, while that of the winter dry season decreases in the opposite direction (Figure 4).

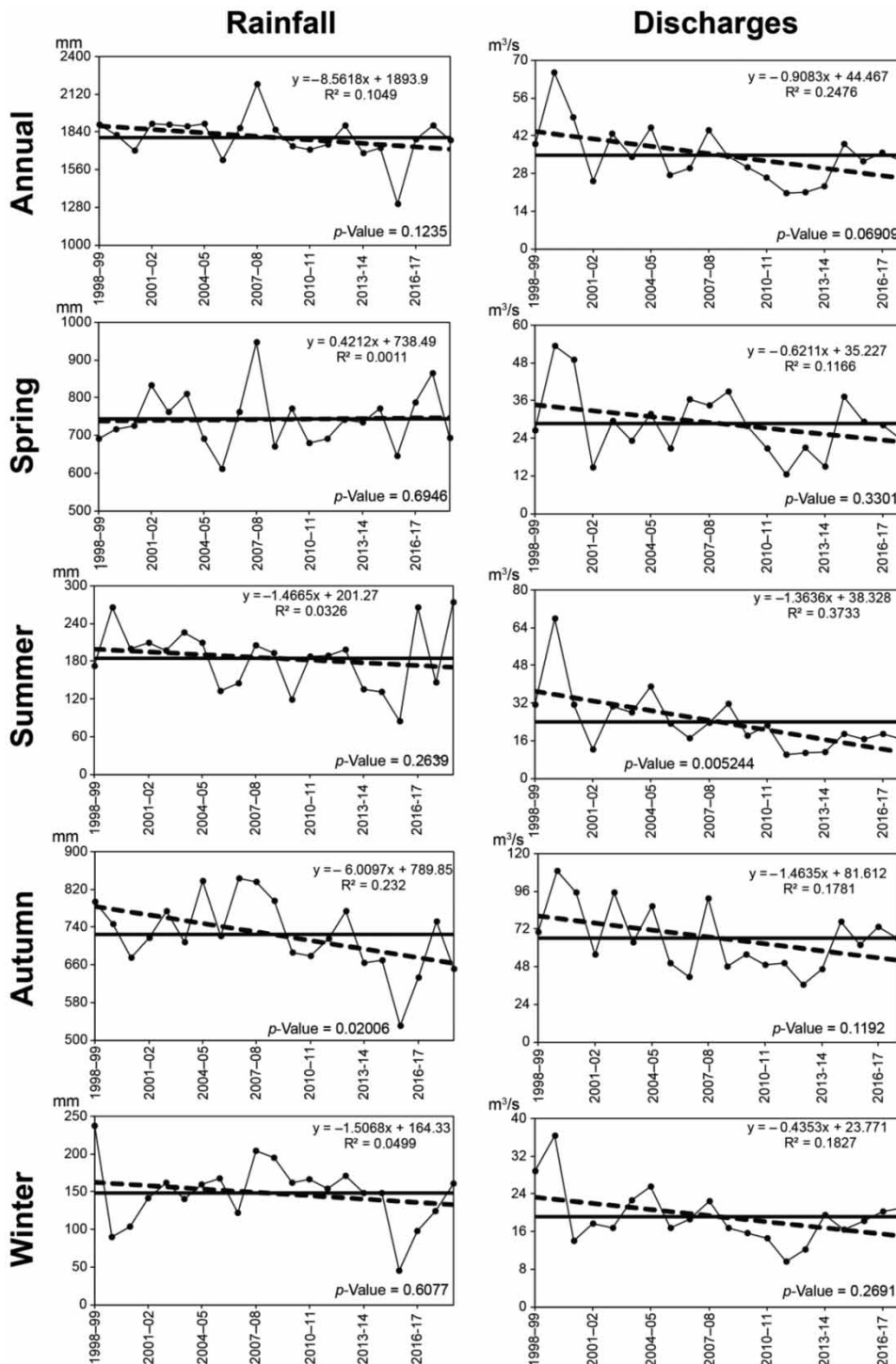


**Figure 3** | Evolution of rainfall and discharges of the So'o catchment at annual and seasonal time steps. The continuous horizontal lines indicate the interannual average. The trends are represented by oblique broken lines.

### 3.1.2. Evolutions of flows

The average annual and seasonal flows of the So'o decreased over the periods 1998–1999 and 2017–2018 (Figure 3). These decreases are all non-significant according to the Pettitt test. The mean summer flows that experienced the largest decrease



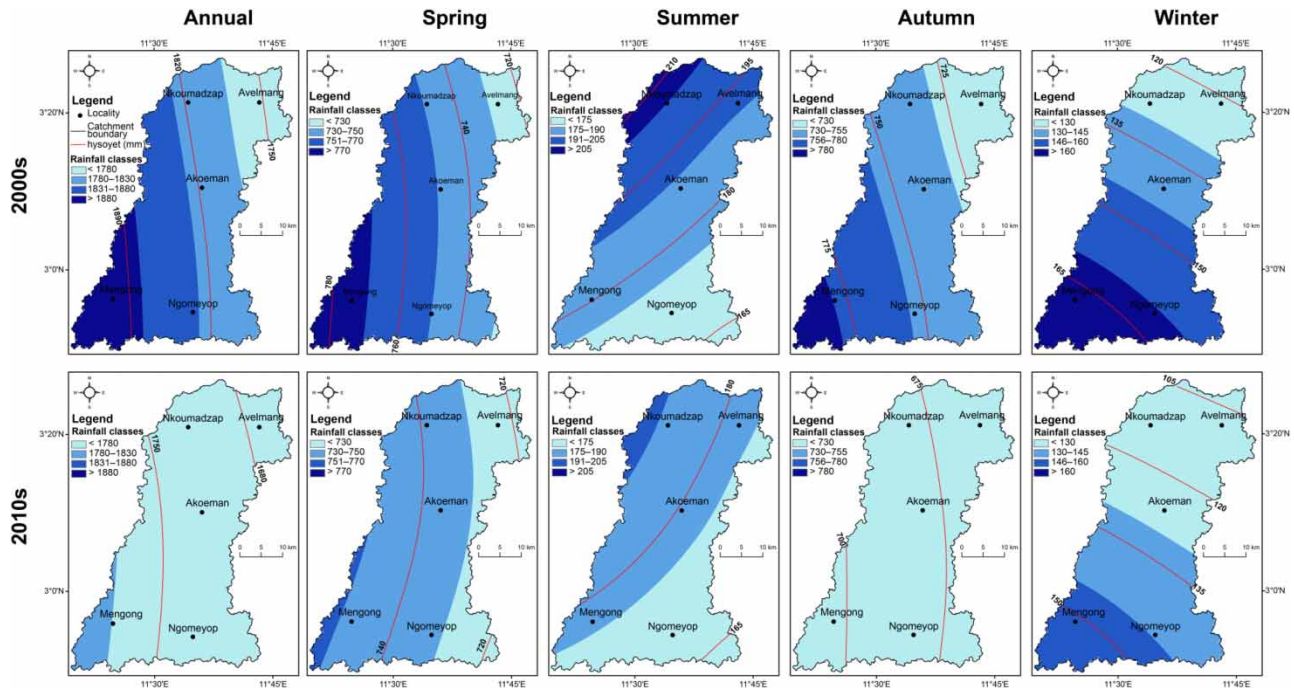


**Figure 4** | Spatial distribution of mean precipitation in the So'o basin at annual and seasonal time steps, between the 1950–1970 and 1980–2010 decades.

are the only ones to have recorded a significant decrease according to the Mann–Kendall test (Figure 3). The smallest decrease in runoff was observed during the spring season.

### 3.1.3. Impact of precipitation on runoff

The impact of rainfall on the evolution of the So'o flows seems quite clear at annual and seasonal time scales. We note for the two compared variables the same evolution during the period 1998–1999 to 2018–2019, which makes it possible to consider a possible role of the decrease in rainfall on runoff. It should be noted, however, that the magnitudes of the decreases in precipitation in the different seasons do not always correspond to those of the runoff in the same seasons. The summer dry season flows, for example, recorded the largest drop, yet it was for the autumn rainfall that the largest drop was observed. This could be linked to the fact that in the equatorial region, the precipitation of certain seasons has an impact on the flows of other seasons, most often those which follow them (Liénoú *et al.* 2008; Ebodé *et al.* 2022).

## 3.2. SWAT model performance

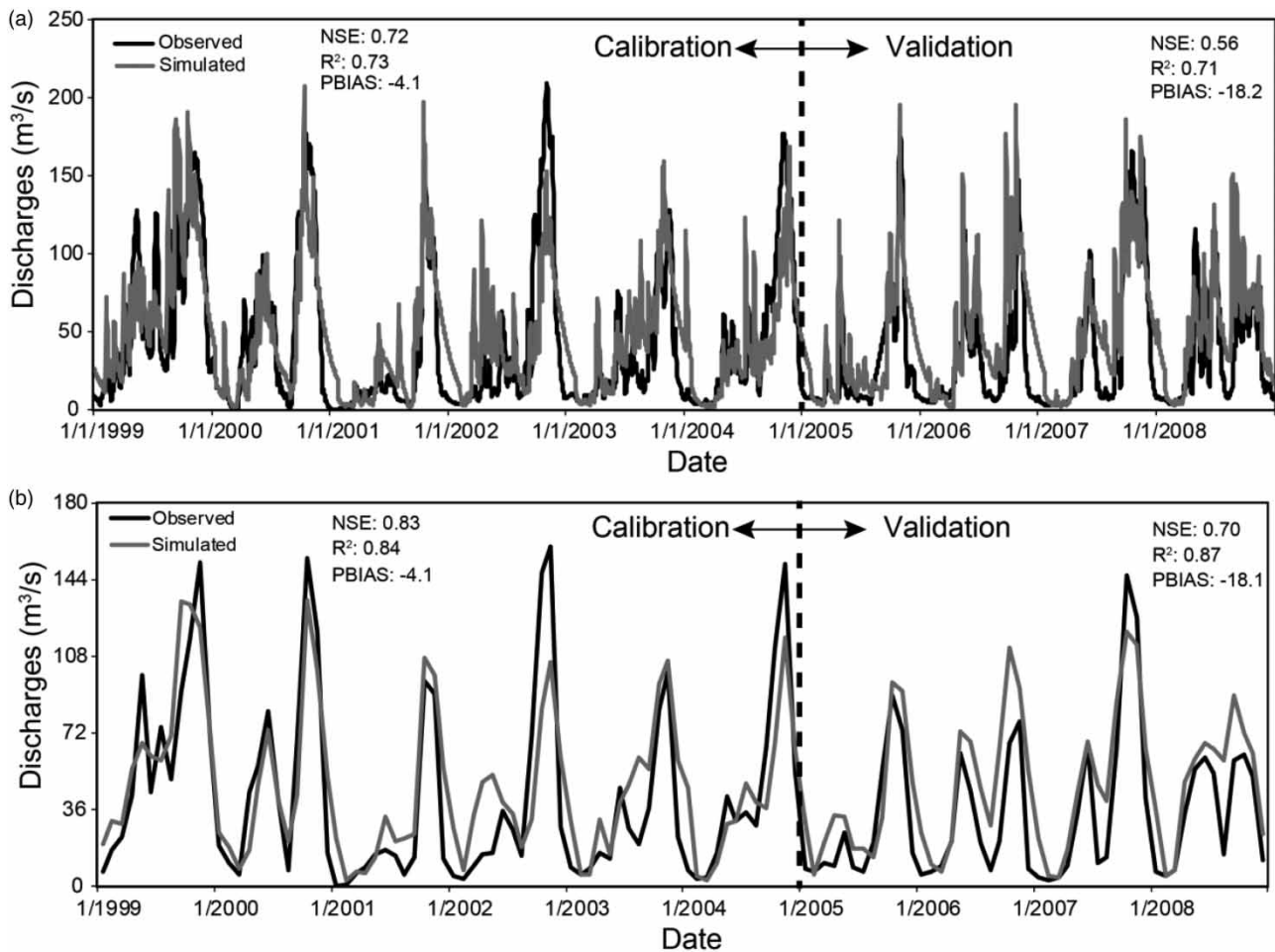
To identify the parameters having a major influence on the outputs of the model, a sensitivity analysis was carried out from the daily flows observed. Initially, four parameters relating globally to runoff and groundwater were identified as being the most sensitive in calibration (Table 1).

The results of SWAT model (version 2012.10.24) calibration (1999–2004) show that the simulated daily and monthly flows agree with those observed at the Pont So'o station (Figure 5). This satisfactory calibration translates monthly into a correlation coefficient, a Nash index and a bias of 0.84, 0.83 and  $-4.1$ , respectively (Figure 5). Concerning validation (2005–2008), the results of the model at this same time step are significantly better than in calibration. This can be seen by a slightly clearer synchronism between the flow rate curves compared. The values of the correlation coefficient, the Nash index and the bias are also satisfactory. They are, respectively, 0.87, 0.70 and  $-18.1$  (Figure 5).

This work confirms the ability of the SWAT model to reproduce flows satisfactorily in the equatorial region. Similar results were obtained elsewhere. For example, Arnold & Allen (1999) have used observed data from three watersheds, ranging in size from 122 to 246 km<sup>2</sup>, to successfully validate flows simulated from SWAT. Other authors (Arnold *et al.* 1999) have also successfully evaluated the ability of the model to reproduce flows in the Gulf of Texas over basin sizes between 2,253 and 304,260 km<sup>2</sup>.

**Table 1** | Sensitivity analysis and calibrated parameters

Parameter name	Sensitivity			Calibration	
	t-Stat	p-Value	Sensitivity range	Parameter value range	Fitted value
r_CN2.mgt (Surface runoff)	0.26	0.8	1	-0.2 to 0.2	-0.14
v_ALPHA_BF.gw (Groundwater)	0.88	0.41	2	0-1	0.25
v_GW_DELAY.gw (Groundwater)	0.76	0.48	3	30-450	135
v_GWQMIN.gw (Groundwater)	0.79	0.46	4	0-2	1.7

**Figure 5** | Calibration and validation of daily (a) and average monthly (b) streamflow of the So'o river at the So'o bridge.

### 3.3. Future hydroclimatic variability

#### 3.3.1. Evolution of the future climate according to RCMs

To highlight the evolution of the future climate, the averages of the corrected precipitation and temperature series for each of the two RCMs (CCCma and RCA4), for each of the two emission scenarios (RCP4.5 and RCP8.5) and for each future period (2022-260 and 2061-2100) were compared with those of the historical period (1999-2008).

**3.3.1.1. Precipitation.** Compared to the historical period, the RCA4 model predicts a decrease in precipitation in the near future (2022-2060) in the SRB, with an increase in the distant future (2061-2100), regardless of the emission scenario

considered (Figures 6 and 7). Over the period 2022–2060, the decreases are projected, respectively, under the RCP4.5 and RCP8.5 scenarios as  $-9.1$  and  $-12.6\%$  (Table 2). According to the model, the decrease in precipitation over this interval will be mainly caused by a decrease in summer and autumn precipitation since the other two seasons (spring and winter) will experience an overall increase (Figure 6). The 2020s and 2030s appear according to the model forecasts are to be the driest of the century under the RCP8.5 scenario. Under the RCP4.5 scenario, this situation concerns the 2020s and 2040s (Figure 7). Between 2061 and 2100, the RCA4 model predicts, unlike the first period (2022–2060), a significant increase in precipitation in the basin under the scenarios RCP4.5 ( $+14.5\%$ ) and RCP8.5 ( $+29.9\%$ ) (Table 2). This increase will mainly result from an increase in winter and spring precipitation (Figure 6). The 2070s and 2090s are projected to be the wettest decades of the century under the RCP8.5 scenario. Under the RCP4.5 scenario, the 2080s and 2090s will be the wettest decades (Figure 7).

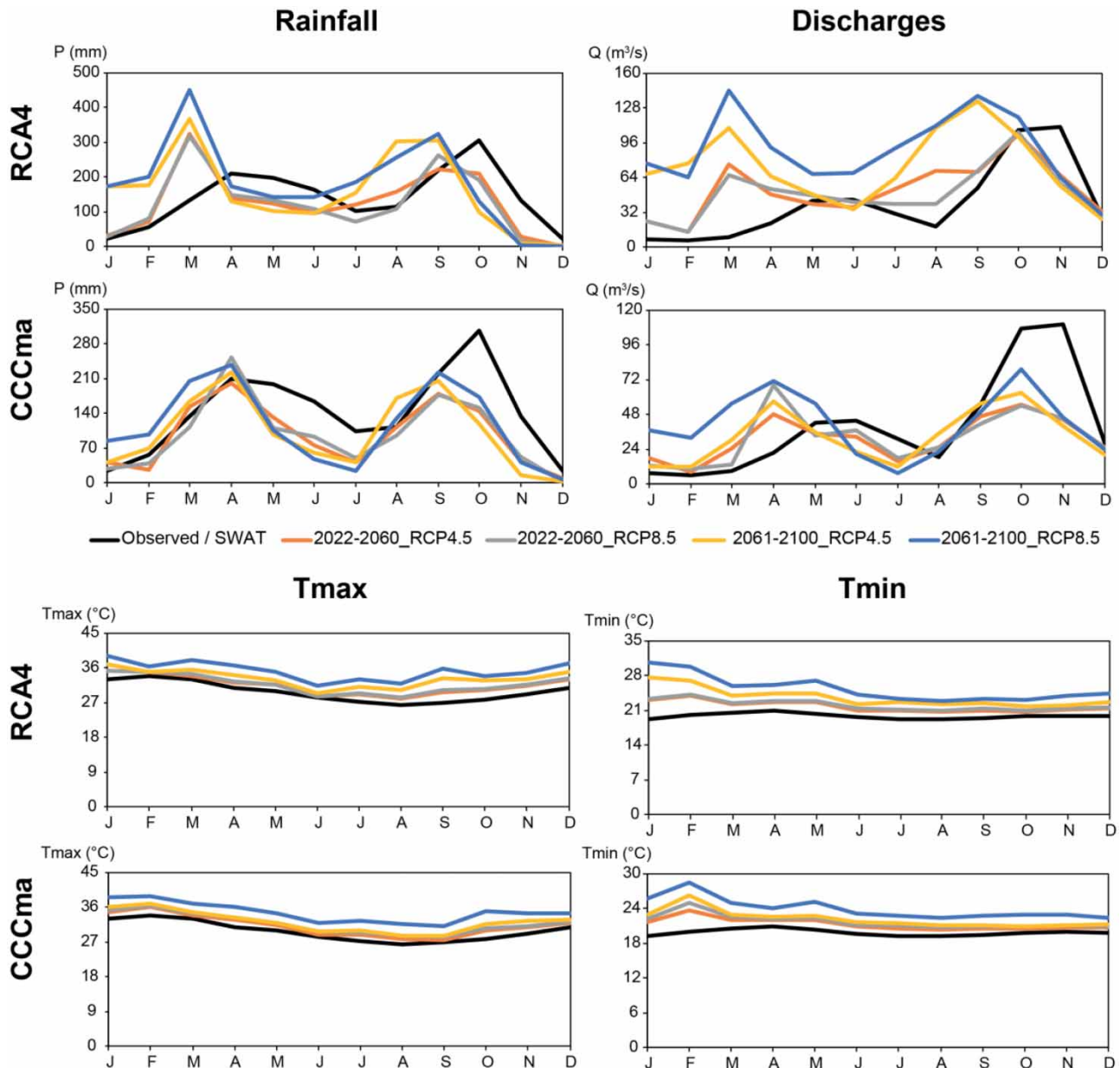


**Figure 6** | Seasonal projected change in mean rainfall, discharges, maximum temperatures and minimum temperatures in the So'o catchment for 2022–2060 and 2061–2100 under the RCP4.5 and RCP8.5 scenarios.

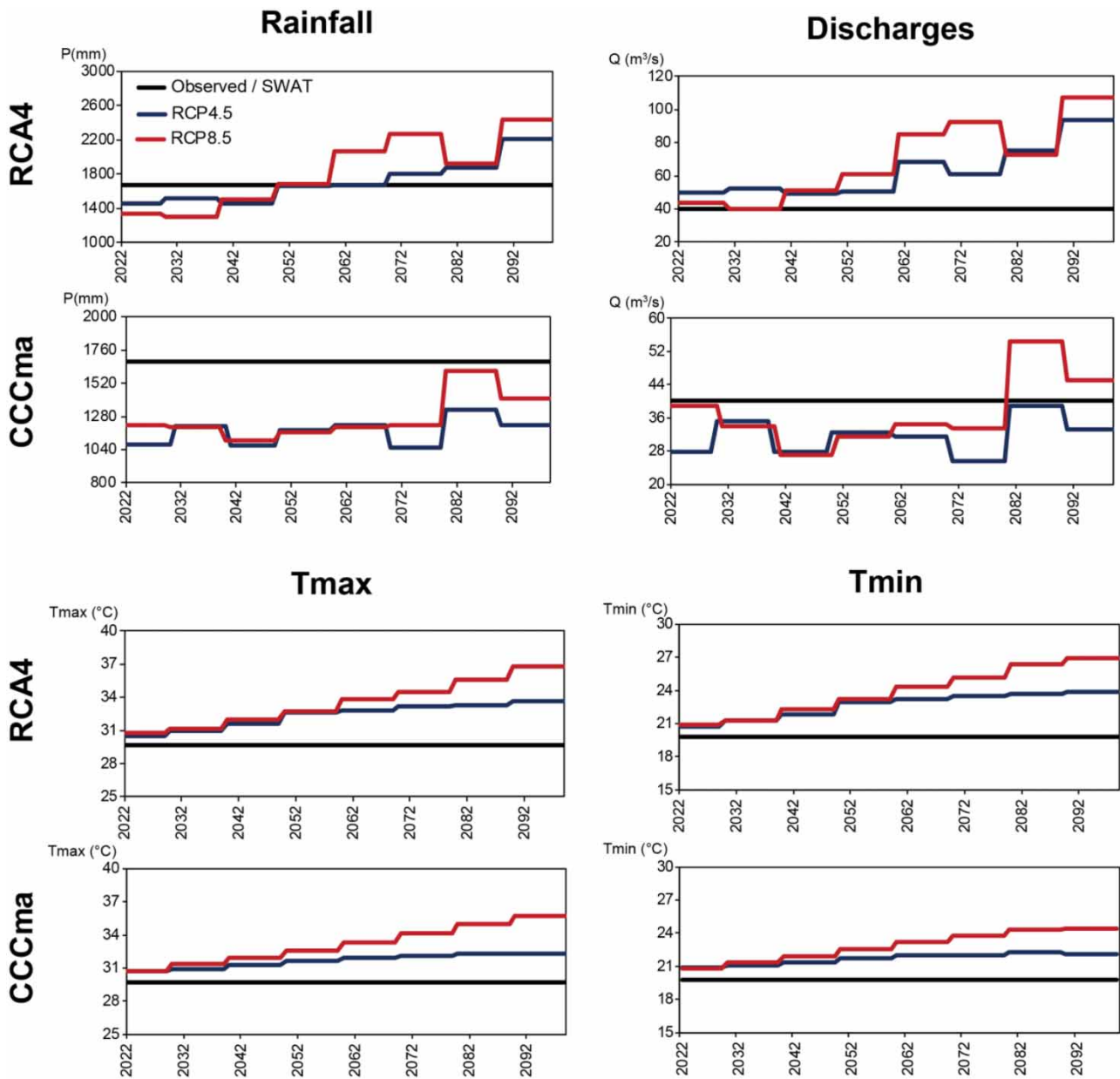


**Figure 7** | Decadal projected change in mean rainfall, discharges, maximum temperatures and minimum temperatures in the So'o catchment for 2022–2100 under the RCP4.5 and RCP8.5 scenarios.

**Table 2** | Changes in rainfall and discharges (%) across the two RCMs in RCP4.5 and RCP8.5 scenarios

RCMs	RCP4.5		RCP8.5	
	2022–2060	2061–2100	2022–2060	2061–2100
Discharges				
RCA4	+31.9	+85.7	+22.8	+122
CCCma	-21.2	-17.9	-20.2	+4
Rainfall				
RCA4	-9.1	+14.5	-12.6	+29.9
CCCma	-31	-27.9	-30.8	-18

In their study of the Finchaa watershed in Ethiopia, *Dibaba et al. (2020)* highlighted a decrease in rainfall from the RCA4 model in the near (2021–2050) and distant (2051–2080) future. This study, however, notes a decrease in precipitation for the same model in the near future only (2022–2060). An increase is projected by the model in the distant future (2061–2100).

The CCCma model predicts a decrease in precipitation in the SRB for both periods and under the two scenarios considered (*Table 2*). For the first period, the decreases are projected to be, respectively, –31 and –30.8% under the RCP4.5 and RCP8.5 scenarios. For the second, respective decreases of –27.9 and –18% are forecast under the RCP4.5 and RCP8.5 scenarios (*Table 2*). This decrease in precipitation will mainly result from that of the summer and autumn precipitation (*Figure 6*). Under the RCP8.5 scenario, the 1940s is the only decade for which the deficit seems more severe compared to the others, three decades present an apparent deficit under the RCP4.5 scenario including the 2020s, 2040s and 2070s (*Figure 7*).

**3.3.1.2. Temperatures.** The two models (RCA4 and CCCma) project an increase in maximum and minimum temperatures, regardless of the period and the scenario considered (*Figure 6* and *Table 3*). In general, this temperature rise will gradually increase over the decades, and only peak towards the end of the century (*Figure 7*). The RCP8.5 scenario also appears to be the one for which the increase is greater, especially after the 1960s (*Table 3* and *Figure 7*). Under the RCP8.5 scenario, the average maximum temperature of the 2100 decade exceeds 35°, regardless of the model considered. However, it does not exceed 32° under the RCP4.5 scenario (*Figure 7*). The observation is practically the same for minimum temperatures. Those predicted by the two models under the RCP8.5 scenario are generally about 2° higher than those predicted under the RCP4.5 scenario during the last two decades of the century. Seasonally, both models predict a larger increase in winter and spring minimum temperatures. For maximum temperatures, on the other hand, the expected increase is almost regular throughout the year (*Figure 6*).

As is the case in this work, several studies dealing with the impact of climate change on resources (*Kingston & Taylor 2010; Basheer et al. 2015*) have already noted in the hydrological units studied a gradual increase in future maximum and minimum temperatures under the different scenarios retained.

### 3.3.2. Future evolution of land use

Three main modes of land use having a direct link with the flow have been identified in the SRB. These are the forest, urban areas and water bodies. The land cover forecasts for the years 2035 and 2065 were certainly made based on the changes noted between 2005 and 2015, but the year 2005 is considered as the reference year from which the probable future land cover changes are assessed.

Changes in surface conditions are noted over the 2005–2035 and 2005–2065 intervals (*Figure 8*). Between 2005 and 2035, there will be a decrease in forest areas of –1.14%. Conversely, we note an increase in urban areas and water bodies of +261.3 and +4%, respectively (*Table 4*). Between 2005 and 2065, developments similar to the previous ones are expected to occur. A decrease in forests (–1.9%) and an increase in urban areas (+355%) and water bodies (+30%) are expected (*Table 1*).

### 3.3.3. Impact of climate change and future anthropization on flows

**3.3.3.1. Impact of climate change.** The predictions of climate models (precipitation and temperature) were integrated into the SWAT model to get an idea of possible future changes in discharges in the SRB.

**Table 3** | Changes in temperatures (°C) across the two RCMs in RCP4.5 and RCP8.5 scenarios

RCMs	RCP4.5		RCP8.5	
	2,022–2,060	2,061–2,100	2,022–2,060	2,061–2,100
$T_{\max}$				
RCA4	+1.8	+3.6	+2	+5.5
CCCma	+1.5	+2.5	+2	+4.9
$T_{\min}$				
RCA4	+1.9	+3.8	+2.2	+5.7
CCCma	+1.5	+2.3	+1.9	+4.1

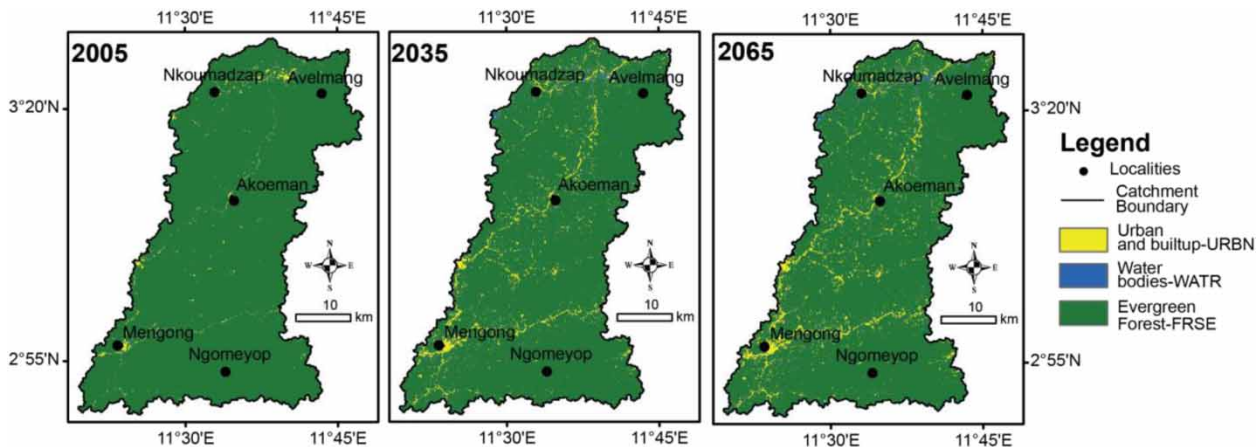


**Figure 8** | Main land use/land cover maps and their SWAT code.

**Table 4** | Evolution of the main land use modes in the So'o watershed

Main land use modes	Surface (km <sup>2</sup> )			Evolution between 2005 and 2035		Evolution between 2005 and 2065	
	2,005	2,035	2,065	km <sup>2</sup>	%	km <sup>2</sup>	%
Evergreen forest-FRSE	1,900.4	1,878.6	1,865.2	-21.8	-1.14	-35.2	-1.9
Urban and builtup-URBN	8	28.9	36.4	+20.9	+261.3	+28.4	+355
Water bodies-WATR	22.6	23.5	29.4	+0.9	+4	+6.8	+30

With regard firstly to the RCA4 model, the results obtained show that a change in precipitation in line with projections will cause an increase in discharges, whatever the period and the scenario taken into account. In general, this increase will be greater during the dry seasons (winter and summer), and the decades at the end of the century will be the wettest (Figures 6 and 7). The changes (increases) noted during the second period (2061–2100) are consistent with those observed for rainfall under the two scenarios (RCP4.5 and RCP8.5). We could also see an effective impact of climate change on flows during this period and under these two scenarios. The climate forecasts of this model do not, however, explain the increase noted during the first period (2022–2060) under the same scenarios. This increase is indeed concomitant with a decrease in precipitation and an increase in temperature. The analysis of the impact of anthropogenic changes and its effects which will be done later in this part of the article will certainly allow us to see more clearly on this subject.

Concerning the CCCma model, a change in precipitation in line with the forecasts of the latter will cause a decrease in the runoff, except under the RCP8.5 scenario during the second period (2061–2100), where we note an increase compared to the historical period of about +4% (Table 2). This decrease will mainly concern the autumn months, and the 2020s, 2040s and 2070s will be the most affected (Figures 5 and 6). The impact of climate change is also visible on the flows simulated from the outputs of the model, for almost all periods and scenarios. It is only for the second period under the RCP8.5 scenario that we observed a different evolution between precipitation (decrease) and flow (increase) (Table 2). This again gives rise to questions about the possible impact of anthropogenic change and its effects on future flows of the So'o.

To ensure better management of water resources, the impact of climate change water resources has been addressed in several studies around the world (Notter *et al.* 2013; Wagena *et al.* 2016; Danvi *et al.* 2018; Duku *et al.* 2018). In these different studies, the outputs of the climate models were integrated into the SWAT model to simulate future flows and get an idea of their possible evolution. As is the case in this study, some of the studies also predict identical trends in the evolution of future precipitation and runoff (Beyene *et al.* 2010; Basheer *et al.* 2015; Dibaba *et al.* 2020).

**3.3.3.2. Impact of surface condition changes.** The explanations for certain changes in the future flows of the So'o watershed could not be justified by projected changes in precipitation and temperature. In this case, the projected changes in simulated

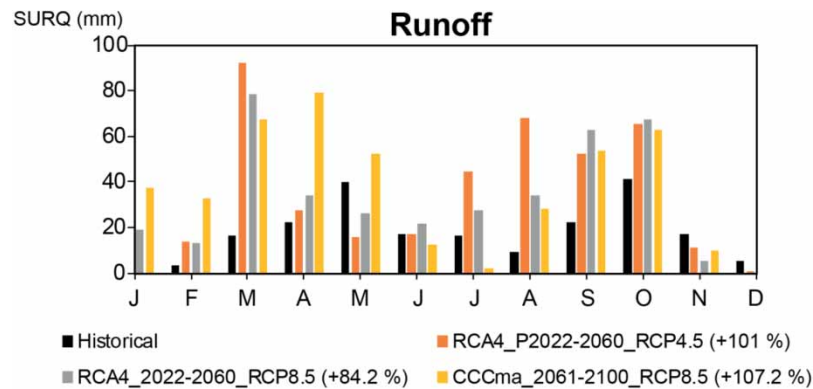


**Figure 9** | Seasonal projected change in the mean runoff in the So'o catchment for the three cases where an increase in future discharges is projected, despite the decline in rainfall and increase in temperature.

flows for the first period (2022–2060) from the RCA4 model under the two scenarios, and the simulated flow for the second period (2061–2100) from the outputs of the CCCma model under the RCP8.5 scenario. In these different scenarios, an increase in discharges has been noted, while rainfall decreases and temperatures increase, which should rather cause a decrease in discharges, due to a reduced supply of the groundwater and increased evapotranspiration. This raises questions about the evolution of surface conditions, knowing that an increase in impermeable spaces, for example, increases runoff and therefore flows.

Let us first recall that in this study, the land cover maps used to simulate flows for the historical period (used to assess changes in future periods) and future periods 2022–2060 and 2061–2100 are, respectively, those for the years 2005, 2035 and 2065. Compared to the situation for the year 2005, the urbanized areas are supposed to experience an increase of +261.3% in 2035 and +355% in 2065 (Table 4). This increase will cause an increase in runoff (Figure 9), which is the only possible explanation for the increase in future flows in the various cases where a drop in precipitation is forecast. The runoff simulated from the outputs of the RCA4 model for the period 2022–2060 is projected to increase compared to that of the historical period by approximately +101% under the RCP4.5 scenario and +84.2% under the RCP8.5 scenario. Under the RCP8.5 scenario, during the period 2061–2100, the runoff simulated from the outputs of the CCCma model is projected to increase by approximately +107.2%. The winter, spring and summer months will be the seasons affected by this increase, whatever the period and the scenario considered (Figure 9).

#### 4. CONCLUSION

The objectives of this study were to evaluate the capacity of the SWAT model to simulate flows in a complex equatorial river basin with two rainy season regimes and to use the model to simulate future flows in the basin under different climate change scenarios. Between 1998–1999 and 2018–2019, the SRB experienced a decrease in discharges caused by a decrease in precipitation. Model simulation using outputs from the CCCma model indicates that flows in this river will decrease more, except under the RCP8.5 scenario during the second period (2061–2100), where flows are projected to increase compared to the historical period by approximately +4%. This decrease will be observed mainly in the autumn months, and the decades 2020, 2040 and 2070 will be the most affected. A change in precipitation according to the projections of the RCA4 model will on the other hand cause an increase in discharges by more than +50%, whatever the period and the scenario. This increase will be greater during the dry seasons (winter and summer), and the decades at the end of the century (2080–2100) will be the wettest. For some cases, an increase in flows was noted despite a drop in rainfall, particularly in the case of flows simulated for the first period from the outputs of the CCCma model. This seems to be a consequence of the increase in urban areas. This is confirmed by the increase in runoff observed during this period.

#### AUTHOR CONTRIBUTIONS

V.B.E., J.G.D. and J.J.B. conceptualized the study and performed the methodology; V.B.E. did software analysis and formal analysis; investigated the study; did data curation; V.B.E., E.N. and J.G.D. wrote and prepared the original draft; V.B.E.,

B.N.N. and E.N. wrote, reviewed and edited the article; project administration by V.B.E. All authors have read and agreed to the published version of the manuscript.

## FUNDING

This research received no external funding.

## DATA AVAILABILITY STATEMENT

Data cannot be made publicly available; readers should contact the corresponding author for details.

## CONFLICT OF INTEREST

The authors declare there is no conflict.

## REFERENCES

- Abbott, M. B., Bathurst, J. C., Cunge, J. A., O'Connell, P. E. & Rasmussen, J. 1986 An introduction to the European hydrological system – système hydrologique européen SHE 2, structure of a physically based distributed modelling system. *Journal of Hydrology* **87**, 61–77. [https://doi.org/10.1016/0022-1694\(86\)90114-9](https://doi.org/10.1016/0022-1694(86)90114-9).
- Abe, C. A., Lobo, F. D., Dibike, Y. B., Costa, M. P., Dos Santos, V. & Novo, E. M. 2018 Modelling the effects of historical and future land cover changes on the hydrology of an amazonian basin. *Water* **10**, 932. <https://doi.org/10.3390/w10070932>.
- Ague, A. I., Afouda, A. & Lanhoussi, F. 2014 Etude comparative d'un modèle conceptuel global (GR4J) et d'un modèle semi-distribué (GéoSFM) sur le bassin versant de l'Ouémé à Savè (Bénin, Afrique de l'Ouest). *Revue Scientifique et Technique* **24**, 1–8.
- Akoko, G., Kato, T. & Tu, L. H. 2020 Evaluation of irrigation water resources availability and climate change impacts – a case study of mwea irrigation scheme, Kenya. *Water* **12** (9), 2330. <https://doi.org/10.3390/w12092330>.
- Akoko, G., Le, T. H., Gomi, T. & Kato, T. 2021 A review of SWAT model application in Africa. *Water* **13**, 1313. <https://doi.org/10.3390/w13091313>.
- Amoussou, E. 2015 *Analyse hydrométéorologique des crues dans le bassin-versant du Mono en Afrique de l'Ouest avec un modèle conceptuel pluie-débit*. FMSH-WP-2015-90.
- Andrade, M. A., Mello, C. R. & Beskow, S. 2013 Simulação hidrológica em uma bacia hidrográfica representativa dos Latossolos na região Alto Rio Grande, MG. *Rev. Engenharia Agrícola E Ambiental* **17**, 69–76.
- Araghi, A., Mousavi Baygi, M., Adamowski, J., Malard, J., Nalley, D. & Hasheminia, S. M. 2014 Using wavelet transforms to estimate surface temperature trends and dominant periodicities in Iran based on gridded reanalysis data. *Atmospheric Research* **155**, 52–72. <https://doi.org/10.1016/j.atmosres.2014.11.016>.
- Ardoïn-Bardin, S. 2004 *Variabilité hydroclimatique et impacts sur les ressources en eau de grands bassins hydrographiques en zone soudano-sahélienne*. Université Montpellier II – Sciences et Techniques du Languedoc, Montpellier, France.
- Arnold, J. G. & Allen, P. M. 1999 Automated methods for estimating baseflow and ground water recharge from streamflow records. *Journal of American Water Resources Association* **35**, 411–424. <https://doi.org/10.1111/j.1752-1688.1999.tb03599.x>.
- Arnold, J. G., Srinivasan, R., Mutiah, R. S. & Williams, J. R. 1998 Large area hydrologic modeling and assessment part I: model development. *Journal of American Water Resources Association* **34**, 73–89. <https://doi.org/10.1111/j.1752-1688.1998.tb05961.x>.
- Arnold, J. G., Srinivasan, R., Ramanarayanan, T. S. & Di Luzio, M. 1999 Water resources of the Texas Gulf basin. *Water Science and Technology* **39** (3), 121–133. [https://doi.org/10.1016/S0273-1223\(99\)00044-X](https://doi.org/10.1016/S0273-1223(99)00044-X).
- Arnold, J. G., Kiniry, J. R., Srinivasan, R., Williams, J. R., Haney, E. B. & Neitsch, S. L. 2012 *Soil and Water Assessment Tool: Input/Output Documentation*. Version 2012, TR-439, Texas Water Resources Institute, College Station, USA.
- Basheer, A., Lü, H., Omer, A., Ali, A. & Abdelgader, A. 2015 Impacts of climate change under CMIP5 RCP scenarios on the streamflow in the dinder river and ecosystem habitats in dinder national park, Sudan. *Hydrology and Earth System Sciences Discussions* **12**, 10157–10195. doi:10.5194/hessd-12-10157-2015.
- Beven, K. J. & Kirkby, M. J. 1979 A physically based, variable contributing area model of basin hydrology. *Hydrological Sciences Bulletin* **24**, 43–69. <https://doi.org/10.1080/02626667909491834>.
- Beyene, T., Lettenmaier, D. P. & Kabat, P. 2010 Hydrologic impacts of climate change on the Nile River Basin: implications of the 2007 IPCC scenarios. *Climatic Change* **100**, 433–461. <https://doi.org/10.1007/s10584-009-9693-0>.
- Bigot, S., Philippon, N., Gond, V., Moron, V., Pokam, W., Bayol, N., Boyemba, F., Kahindo, B., Samba, G., Ngomanda, A., Gapia, M., Yongo, O. D., Laurent, J.-P., Gourlet-Fleury, S., Doumoungé, C., Forni, E., Camberlin, P., Martiny, N., Dubreuil, V. & Brou, T. 2016 Etat actuel des réseaux de mesure éco-climatiques en Afrique centrale : Les ambitions du projet de recherche internationale FORGREENE. In: *XXIX Colloque de L'Association Internationale de Climatologie*, Lausanne – Besançon, Suisse.
- Bodian, A., Dezetter, A. & Dacosta, A. 2012 Apport de la modélisation pluie-débit pour la connaissance de la ressource en eau : application au haut Bassin du Fleuve Sénégal. *Climatologie* **9**, 109–125. <https://doi.org/10.4267/climatologie.223>.



- Bodian, A., Diop, L., Panthou, G., Dacosta, H., Deme, A., Dezetter, A., Ndiaye, P. M., Diouf, I. & Vischel, T. 2020 Recent trend in hydroclimatic conditions in the Senegal River Basin. *Water* **12**, 436. <https://doi.org/10.3390/w12020436>.
- Boyle, D. P., Gupta, H. V., Soroshian, S., Koren, V., Zhang, Z. & Smith, M. 2001 Toward improved streamflow forecasts: value of semidistributed modeling. *Water Research* **37**, 2749–2759. [https://doi.org/10.1016/S1464-1909\(99\)00081-7](https://doi.org/10.1016/S1464-1909(99)00081-7).
- Cao, W., Bowden, W. B., Davie, T. & Fenemor, A. 2006 Multi-variable and multi-site calibration and validation of SWAT in a large mountainous catchment with high spatial variability. *Hydrological Processes* **20**, 1057–1073. <https://doi.org/10.1002/hyp.5933>.
- Cissé, M. T., Sambou, S., Dieme, Y., Diatta, C. & Bop, M. 2014 Analyse des écoulements dans le bassin du fleuve Sénégal de 1960 à 2008. *Revue des Sciences de L'eau* **27** (2), 167–187. <https://doi.org/10.7202/1025566ar>.
- Collischonn, W. & Tucci, C. E. M. 2001 Simulação hidrológica de grandes bacias. *Revista Brasileira de Recursos Hidricos* **6**, 95–118.
- Conway, D. P., Persechini, A., Ardoin-Bardin, S., Hamandawana, H., Dieulin, C. & Mahé, G. 2009 Rainfall and river flow variability in sub-saharan Africa during the 20th century. *Journal of Hydrology* **10**, 41–59.
- Danvi, A., Giertz, S., Zwart, S. J. & Diekkriiger, B. 2018 Rice intensification in a changing environment: impact on water availability in inland valley landscapes in Benin. *Water* **10** (1), 74. <https://doi.org/10.3390/w10010074>.
- Descroix, L., Sané, Y., Thior, M., Manga, S. P., Ba, B. D., Mingou, J., Mendy, V., Coly, S., Dièye, A., Badiane, A., Senghor, M. J., Diedhiou, A. B., Sow, D., Bouaita, Y., Soumaré, S., Diop, A., Faty, B., Sow, B. A. Machu, E., Montoroi, J. P., Andrieu, J. & Vandervaere, J. P. 2020 Inverse estuaries in West Africa: evidence of the rainfall recovery? *Water* **12**, 647. <https://doi.org/10.3390/w12030647>.
- Dibaba, W. T., Miegel, K. & Demissie, T. A. 2019 Evaluation of the CORDEX regional climate models performance in simulating climate conditions of two catchments in Upper Blue Nile Basin. *Dynamics of Atmospheres and Oceans* **87**, 101104. doi:10.1016/j.dynatmoce.2019.101104.
- Dibaba, W. T., Demissie, T. A. & Miegel, K. 2020 Watershed hydrological response to combined land Use/Land cover and climate change in highland Ethiopia: finchaa catchment. *Water* **12**, 1801. <https://doi.org/10.3390/w12061801>.
- Diem, J. E., Hill, T. C. & Milligan, R. A. 2018 Diverse multi-decadal changes in streamflow within a rapidly urbanizing region. *Journal of Hydrology* **556**, 61–71. <https://doi.org/10.1016/j.jhydrol.2017.10.026>.
- Diermanse, F. 1999 Representation of natural heterogeneity in rainfall-runoff models. *Physics and Chemistry of the Earth B* **24**, 787–792.
- Dile, Y. T., Berndtsson, R. & Setegn, S. G. 2013 Hydrological response to climate change for Gilgel Abay River, in the Lake Tana Basin – upper blue Nile basin of Ethiopia. *PLoS ONE* **8**, e79296. <https://doi.org/10.1371/journal.pone.0079296>.
- Duku, C., Zwart, S. J. & Hein, L. 2018 Impacts of climate change on cropping patterns in a tropical, sub-humid watershed. *PLoS ONE* **13** (3), e0192642. <https://doi.org/10.1371/journal.pone.0192642>.
- Ebodé, V. B., Mahé, G., Dzana, J. G. & Amougou, J. A. 2020 Anthropization and climate change: impact on the discharges of forest watersheds in Central Africa. *Water* **12**, 2718. <https://doi.org/10.3390/w12102718>.
- Ebodé, V. B., Mahé, G. & Amoussou, E. 2021a Impact de la variabilité climatique et de l'anthropisation sur les écoulements de la Bénoué (nord Cameroun). *Proceedings of the International Association of Hydrological Sciences* **384**, 261–267. <https://doi.org/10.5194/piahs-384-261-2021>.
- Ebodé, V. B., Mahé, G. & Amoussou, E. 2021b Changement climatique dans le bassin versant de l'Ogooué : évolution récente et impact sur les écoulements. *Proceedings of the International Association of Hydrological Sciences* **384**, 247–253. <https://doi.org/10.5194/piahs-384-247-2021>.
- Ebodé, V. B., Braun, J. J., Nnomo, B. N., Mahé, G., Nkiaka, E. & Riotte, J. 2022 Impact of rainfall variability and land Use change on river discharge in south Cameroon. *Water* **14**, 941. <https://doi.org/10.3390/w14060941>.
- Fentaw, F., Hailu, D., Nigussie, A. & Melesse, A. M. 2018 Climate change impact on the hydrology of Tekeze Basin, Ethiopia: projection of rainfall-runoff for future water resources planning. *Water Conservation Science and Engineering* **3**, 267–278. <https://doi.org/10.1007/s41101-018-0057-3>.
- Fuka, D. R., Walter, M. T., MacAlister, C., Degaetano, A. T., Steenhuis, T. S. & Easton, Z. M. 2013 Using the climate forecast system reanalysis as weather input data for watershed models. *Hydrological Processes* **28** (22), 5613–5623. doi:10.1002/hyp.10073.
- Gadissa, T., Nyadawa, M., Behulu, F. & Mutua, B. 2018 The effect of climate change on loss of lake volume: case of sedimentation in Central Rift Valley Basin, Ethiopia. *Hydrology* **5** (4), 67. <https://doi.org/10.3390/hydrology5040067>.
- Githui, F., Mutua, F. & Bauwens, W. 2009 Estimating the impacts of land-cover change on runoff using the soil and water assessment tool (SWAT): case study of Nzoia catchment, Kenya. *Hydrological Sciences Journal* **54**, 899–908. <https://doi.org/10.1623/hysj.54.5.899>.
- Halmy, M. W. A., Gessler, P. E., Hicke, J. A. & Salem, B. B. 2015 Land use/land cover change detection and prediction in the north-western coastal desert of Egypt using Markov-CA. *Applied Geography* **63**, 101–112. doi:10.1016/j.apgeog.2015.06.015.
- Hirsch, R. M. & Slack, J. R. 1984 A nonparametric trend test for seasonal data with serial dependence. *Water Resources Research* **20**, 727–732. <https://doi.org/10.1029/WR020i006p00727>.
- Kingston, D. G. & Taylor, R. G. 2010 Sources of uncertainty in climate change impacts on river discharge and groundwater in a headwater catchment of the Upper Nile Basin, Uganda. *Hydrology and Earth System Sciences* **14**, 1297–1308. <https://doi.org/10.5194/hess-14-1297-2010>.
- Kokkonen, T. S. & Jakeman, A. J. 2001 A comparison of metric and conceptual approaches in rainfall-runoff modeling and its implications. *Water Resources* **37**, 2345–2352. <https://doi.org/10.1029/2001WR000299>.
- Krysanova, V., Bronstert, A. & Mullerwohlfeil, D. L. 1999 Modelling river discharge for large drainage basins: from lumped to distributed approach. *Hydrological Science Journal* **44**, 313–331. <https://doi.org/10.1080/02626669909492224>.

- Legesse, D., Vallet-Coulomb, C. & Gasse, F. 2003 Hydrological response of a catchment to climate and land use changes in Tropical Africa: case study south central Ethiopia. *Journal of Hydrology* **275**, 67–85. [https://doi.org/10.1016/S0022-1694\(03\)00019-2](https://doi.org/10.1016/S0022-1694(03)00019-2).
- Letouzey, R. 1985 *Notice de la Carte Phytogéographique du Cameroun au 1/500000*. Institut de la carte internationale de la végétation, Toulouse, France.
- Liéno, G., Mahé, G., Paturel, J. E., Servat, E., Sighomnou, D., Ekodeck, G. E., Dezetter, A. & Dieulin, C. 2008 Evolution des régimes hydrologiques en région équatoriale camerounaise: un impact de la variabilité climatique en zone équatoriale? *Hydrological Sciences Journal* **53**, 789–801. <https://doi.org/10.1623/hysj.53.4.789>.
- Michaud, J. & Soroshian, S. 1994 Comparison of simple versus complex distributed runoff models on a midsized semiarid watershed. *Water Research* **30**, 593–605. <https://doi.org/10.1029/93WR03218>.
- Neitsch, S. L., Arnold, J. G., Kiniry, J. R. & Williams, J. R. 2005 *Soil and Water Assessment Tool: Theoretical Documentation*. USDA, Agricultural Research Service, Blackland Research Center, Texas A&M University, USA, p. 494.
- Nkiaka, E., Nawaz, N. R. & Lovett, J. C. 2017 Evaluating global reanalysis datasets as input for hydrological modelling in the Sudano-Sahel region. *Hydrology* **4** (1), 13. doi:10.3390/hydrology4010013.
- Notter, B., Hurni, H., Wiesmann, U. & Ngana, J. O. 2013 Evaluating watershed service availability under future management and climate change scenarios in the Pangani Basin. *Physics and Chemistry of the Earth, Parts A/B/C* **61–62**, 1–11. doi:10.1016/j.pce.2012.08.017.
- Olivry, J. C. 1986 *Fleuves et Rivières du Cameroun*. MESRES-ORSTOM, Paris, France.
- Oudin, L., Salavati, B., Furusho-Percot, C., Ribstein, P. & Saadi, M. 2018 Hydrological impacts of urbanization at the catchment Scale. *Journal of Hydrology* **559**, 774–786. <https://doi.org/10.1016/j.jhydrol.2018.02.064>.
- Payraudeau, S. 2002 *Modélisation Distribuée des Flux D'azote sur des Petits Bassins Versants Méditerranéens*. ENGREF, Paris, France.
- Perrin, C., Michel, C. & Andreassian, V. 2003 Improvement of a parsimonious model for streamflow simulation. *Journal of Hydrology* **279**, 275–289.
- Pereira, D. R., Mello, C. R., Silva, A. M. & Yanagi, S. M. N. 2010 Evapotranspiration and estimation of aerodynamic and stomatal conductance in a fragment of Atlantic Forest in Mantiqueira Range region, MG. *Cerne* **16**, 32–40.
- Pettitt, A. N. 1979 A non-parametric approach to the change-point problem. *Applied Statistics* **28** (2), 126–135.
- Rathjens, H., Bieger, K., Srinivasan, R., Chaubey, I. & Arnold, J. G. 2016 *CMhyd User Manual*. Available from: <http://swat.tamu.edu/software/cmhyd/> (accessed on 4 January 2021).
- Sighomnou, D. 2004 *Analyse et Redéfinition des Régimes Climatiques et Hydrologiques du Cameroun : Perspectives D'évolution des Ressources en eau*. Thèse de Doctorat d'Etat, Université de Yaoundé I, p. 290.
- Taleb, R. B., Naimi, M., Chikhaoui, M., Raclot, D. & Sabir, M. 2019 Evaluation Des Performances Du Modele AgroHydrologique SWAT à Reproduire Le Fonctionnement Hydrologique Du Bassin Versant Nakhla (Rif occidental, Maroc). *European Scientific Journal* **15**, 311–333. Doi:10.19044/esj.2019.v15n5p311.
- Tegegne, G., Park, D. K. & Kim, Y. O. 2017 Comparison of hydrological models for the assessment of water resources in a data-scarce region, the Upper Blue Nile River Basin. *Journal of Hydrology: Regional Studies* **14**, 49–66. <https://doi.org/10.1016/j.ejrh.2017.10.002>.
- Teutschbein, C. & Seibert, J. 2012 Bias correction of regional climate model simulations for hydrological climate-change impact studies: review and evaluation of different methods. *Journal of Hydrology* **456–457**, 12–29. doi:10.1016/j.jhydrol.2012.05.052.
- Von Stackelberg, N. O., Chescheir, G. M., Skaggs, R. W. & Amatya, D. M. 2007 Simulation of the hydrologic effects of afforestation in the Tacuarembó River Basin, Uruguay. *Trans. ASABE* **50**, 455–468.
- Wagena, M. B., Sommerlot, A., Chikhaoui, M., Raclot, D. & Sabir, M. 2016 Climate change in the blue Nile basin Ethiopia: implications for water resources and sediment transport. *Climatic Change* **139**, 229–243. <https://doi.org/10.1007/s10584-016-1785-z>.
- Wang, S., Zhang, Z., Sun, G., Strauss, P., Guo, J., Tang, Y. & Yao, A. 2012 Multi-site calibration validation, and sensitivity analysis of the MIKE SHE model for alarge watershed in northern China. *Hydrology and Earth System Sciences* **16**, 4621–4632. <https://doi.org/10.5194/hess-16-4621-2012>.
- Wending, J. 1992 *Modélisation Pluie-Débit en Zone Méditerranéenne: Comparaison D'approches Globales/Distribuées, Conceptuelles/Physico-Déterministes: Essai de Prise en Compte de la Variabilité Spatiale des Pluies (Application au Bassin Versant du Réal Collobrier)*. Thèse de doctorat, Institut National Polytechnique de Grenoble, France.
- Yang, C., Wu, G., Chen, J., Li, Q., Ding, K., Wang, G. & Zhang, C. 2019 Simulating and forecasting spatio-temporal characteristic of land-use/cover change with numerical model and remote sensing: a case study in Fuxian Lake Basin, China. *European Journal of Remote Sensing* **52** (1), 374–384. doi:10.1080/22797254.2019.1611387.
- Zhang, B., Shrestha, N. K., Daggupati, P., Rudra, R., Shukla, R., Kaur, B. & Hou, J. 2018 Quantifying the impacts of climate change on streamflow dynamics of two major rivers of the Northern Lake Erie Basin in Canada. *Sustainability* **10** (8), 2897. <https://doi.org/10.3390/su10082897>.

First received 20 April 2022; accepted in revised form 29 August 2022. Available online 9 September 2022